

Cite this: *Chem. Sci.*, 2025, 16, 14710 All publication charges for this article have been paid for by the Royal Society of ChemistryReceived 30th May 2025  
Accepted 6th July 2025

DOI: 10.1039/d5sc03944d

rsc.li/chemical-science

# Synthesis and immunological evaluation of the lipopolysaccharide outer core of *Salmonella* for potential broad-spectrum protection against multiple *Salmonella* serovars†

Xingling Pan,<sup>ab</sup> Ting-An Chen,<sup>a</sup> Fatemeh Shafieichaharberoud,<sup>ab</sup> Sharon M. Tennant,<sup>c</sup> Scott M. Baliban<sup>c</sup> and Xuefei Huang<sup>b</sup> \*<sup>abd</sup>

*Salmonella* species (*Salmonella* spp.) are a major foodborne pathogen and a leading cause of gastroenteritis in humans. The emergence and continued spread of multidrug-resistant *Salmonella* spp. suggest the urgent need for novel vaccines to complement antibiotics. Currently, there are no approved vaccines against *Salmonella* spp. for human use beyond those for *Salmonella enterica* (*S. enterica*) serovar Typhi. To address this gap, oligosaccharides corresponding to the lipopolysaccharide (LPS) outer core of *S. enterica* were investigated as potential antigens that can target multiple pathogenic *Salmonella* serovars. An efficient chemical synthesis strategy was developed to stereoselectively construct the sterically congested outer core pentasaccharides with five 1,2-*cis* glycosidic linkages. These synthetic glycan antigens were conjugated to the mutant bacteriophage Q $\beta$ , a highly immunogenic carrier system. The resulting constructs elicited strong and durable anti-glycan IgG antibodies, which can robustly bind to *Salmonella* spp. with truncated LPS (rough strain). For smooth strains bearing long LPS chains, the combination of the antisera with the antimicrobial peptide thanatin, an inhibitor of the LPS transport system, exhibited enhanced cytotoxicity toward multiple serovars of pathogenic *Salmonella*, suggesting that combination therapy may serve as a strategy for enhancing protection against salmonellosis.

## Introduction

*Salmonella* is a genus of Gram-negative, facultatively intracellular anaerobes responsible for a range of diseases from localized infections and gastroenteritis to invasive disease including bacteremia and enteric fever. There are multiple types of *Salmonella* species (*Salmonella* spp.) that are pathogenic in humans, including *Salmonella enterica* serovar Typhi (*S. Typhi*), *Salmonella* Paratyphi A, B and C (*S. Paratyphi* A, B and C), and non-typhoidal *Salmonella* (NTS) such as *Salmonella* Enteritidis (*S. Enteritidis*) and *Salmonella* Typhimurium (*S. Typhimurium*). Healthy individuals typically contract *Salmonella* spp. through ingestion of contaminated food or water.<sup>1</sup> Globally, *Salmonella* spp. are among the most common foodborne bacterial

pathogens, causing an estimated 200 million to 1 billion infections annually, including 93 million cases of gastroenteritis and 155 000 deaths.<sup>2–4</sup> In the United States, *Salmonella*-related foodborne illnesses were estimated to cost \$17.1 billion in 2023, making it the most costly among the 31 major foodborne pathogens.<sup>5</sup>

Antibiotics are the main strategy to treat severe *Salmonella* infections. However, drug resistant *Salmonella* strains have become prevalent worldwide.<sup>6–8</sup> For example, analysis of 16 *S. Typhimurium* strains isolated from Nepal showed all isolates were resistant to ampicillin, nalidixic acid, tetracycline, cotrimoxazole and chloramphenicol.<sup>9</sup> In the US, out of 246 *S. Paratyphi* A isolates, 94% were resistant to nalidixic acid or less susceptible to ciprofloxacin.<sup>10</sup> The Centers for Disease Control and Prevention (CDC) has classified drug resistant *Salmonella* including typhoidal and NTS strains as a serious threat, requiring “prompt and sustained action to ensure the problem does not grow”.<sup>11</sup> Vaccines can be an attractive approach to prevent *Salmonella* infections. To date, the only licensed *Salmonella* vaccines in humans target *S. Typhi*.<sup>12–17</sup> No vaccines are yet available against the other major, disease-causing serovars including *S. Paratyphi* A, *S. Typhimurium*, and *S. Enteritidis*.

<sup>a</sup>Department of Chemistry, Michigan State University, 578 South Shaw Lane, East Lansing, MI 48824, USA. E-mail: huangxu2@msu.edu

<sup>b</sup>Institute for Quantitative Health Science & Engineering, Michigan State University, 578 South Shaw Lane, East Lansing, MI 48824, USA

<sup>c</sup>Center for Vaccine Development and Global Health, University of Maryland School of Medicine, Baltimore, 685 W. Baltimore St., Baltimore, MD 21201, USA

<sup>d</sup>Department of Biomedical Engineering, Michigan State University, East Lansing, MI 48824, USA

† Electronic supplementary information (ESI) available. See DOI: <https://doi.org/10.1039/d5sc03944d>



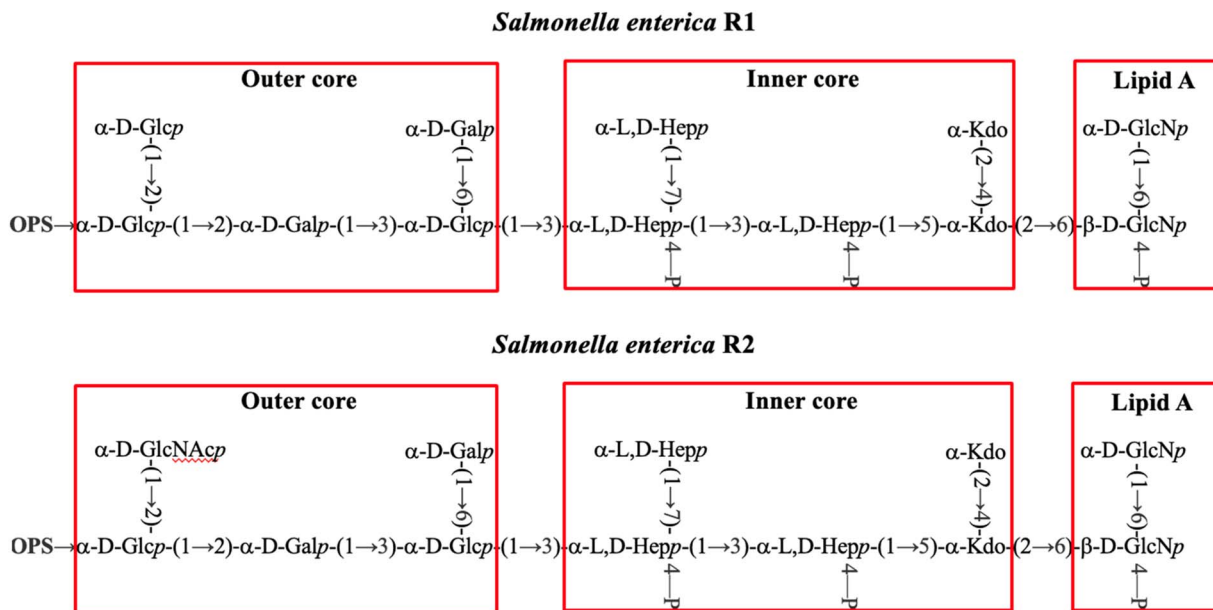


Fig. 1 Chemical structures of *Salmonella* LPS including *S. enterica* subsp. IIIa (R1) and *S. enterica* subsp. I (R2).

Surface polysaccharides are suitable antigens for *Salmonella* vaccine development as exemplified by typhoid conjugate vaccines, which utilize the Vi capsular polysaccharide as the sole vaccine antigen with high success rates in preventing typhoid fever in children after a single dose.<sup>14–16</sup> However, one major drawback in targeting such polysaccharides is that the polysaccharides are often serovar-specific. For example, Vi capsular polysaccharide-based conjugate vaccines are ineffective against Vi-negative *S. Typhi* strains as well as *S. Paratyphi* A, *S. Typhimurium*, or *S. Enteritidis*, since these *Salmonella* serovars do not express Vi. Similarly, the efficacy of a surface carbohydrate based vaccine derived from *S. Enteritidis* would be expected to have limited efficacy against serovars such as *S. Typhimurium* or *S. Paratyphi* A, which express different O-antigen structures.<sup>18–22</sup> Therefore, in order to develop effective vaccines against the major pathogenic serovars of *Salmonella*, a combination of multiple polysaccharide vaccines would be needed, which presents significant hurdles for vaccine development. It would be highly desirable if a common antigen can be established that can enable the targeting of multiple serogroups of *Salmonella*.

As a Gram-negative bacterium, *Salmonella* abundantly expresses lipopolysaccharide (LPS) on the cell surface. Vaccines targeting LPS have demonstrated strong pre-clinical efficacy against various microbial infections, as host recognition of LPS is crucial for clearing Gram-negative bacterial infections.<sup>23–27</sup> The structure of *Salmonella* LPS includes a lipid A moiety (endotoxin), which is embedded in the outer membrane, a conserved core oligosaccharide that bridges lipid A to an extended and highly variable O-polysaccharide (OPS) (Fig. 1 and S1†). Previously, we synthesized OPS-like antigens from *S. Paratyphi* A and *S. Enteritidis*, which were then conjugated with bacteriophage Q $\beta$  to create conjugate vaccines.<sup>21,22</sup> The resulting immune sera provided substantial protection to mice against

lethal challenge with the respective *Salmonella* strain, showcasing the potential efficacy of this synthetic glycan-based vaccine approach. However, the OPS chains exhibit significant variations in both structure and composition, contributing to the extensive diversity of serotypes.<sup>28,29</sup> This variability makes anti-OPS vaccines inherently strain-specific and unable to provide protection against multiple *Salmonella* serotypes bearing different OPS structures.

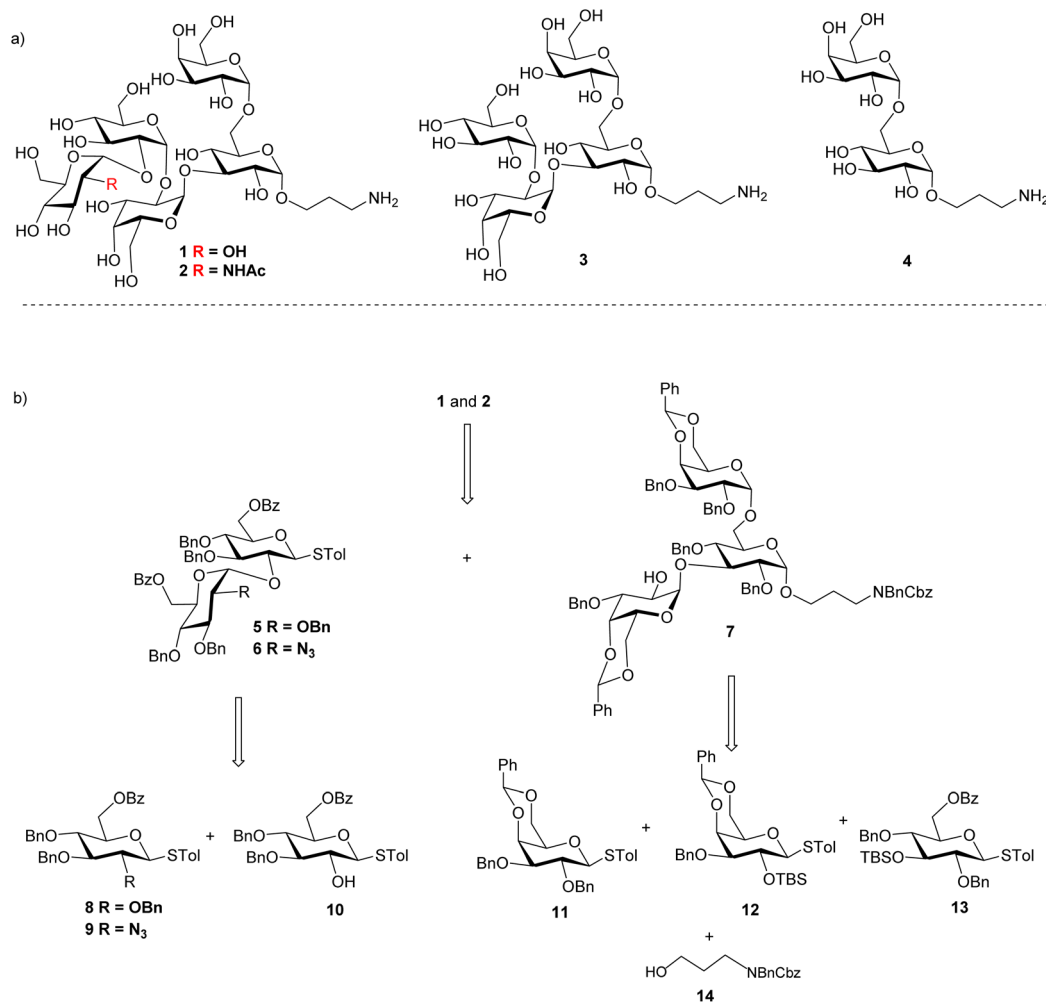
The limitation associated with targeting OPS prompted us to explore the LPS core region as a potential target for vaccine development. The *Salmonella* LPS core displays two chemotypes (R1 and R2) (Fig. 1 and S1†)<sup>28,30</sup> with an outer region and an inner region linked to lipid A. The inner core and lipid A structures are well-conserved across different species within the Enterobacteriaceae family, including *Escherichia coli* (*E. coli*) and *Salmonella* spp.<sup>31</sup> Immunization with a lipo-oligosaccharide containing the inner core and lipid A<sup>32</sup> may cause cross-reactivities with commensal bacteria such as *E. coli*. In comparison, the outer core sequence is unique to each species. To establish a vaccine that can potentially target multiple types of *Salmonella* without affecting commensal bacteria, we decided to focus our investigation on the unique outer core structure of *Salmonella*. Herein, we report the chemical synthesis and immunological evaluation of the outer core domain of *Salmonella* LPS to target multiple types of pathogenic *Salmonella*.

## Results and discussion

### Stereoselective synthesis of *Salmonella* LPS outer core-like pentasaccharides 1 and 2

As it is difficult to purify the LPS outer core from bacteria, chemical synthesis is critical to prepare the LPS glycans for bioconjugation. We focused on the outer core pentasaccharides 1 and 2 from chemotypes R1 and R2 respectively, as well as their



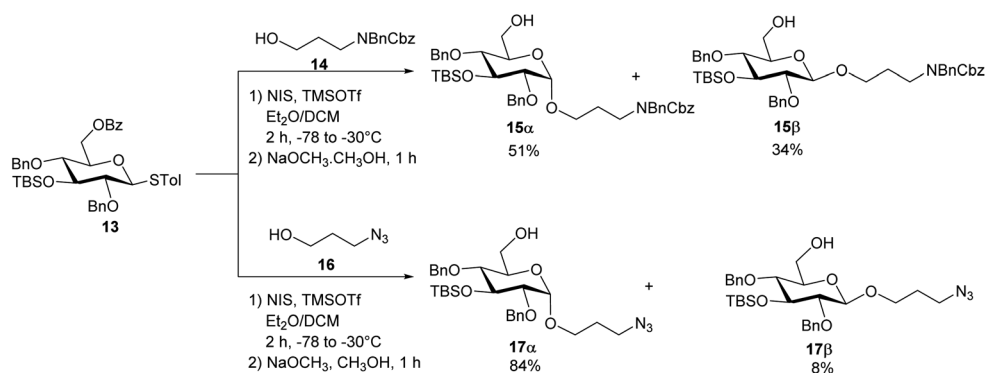


Scheme 1 (a) Structures of *Salmonella* outer core-like glycan targets 1–4; and (b) retrosynthetic analysis of pentasaccharides 1 and 2.

structural fragments, *i.e.*, tetrasaccharide 3 and disaccharide 4. The pentasaccharides 1 and 2 are challenging targets as they contain five 1,2-*cis* linkages (Scheme 1a). Furthermore, the non-reducing end trisaccharides are connected *via* two consecutive  $\alpha$ -1-2 linkages, posing severe steric hindrance to glycosidic bond formation. Our initial strategy for syntheses of pentasaccharides 1 and 2 was based on a [2 + 3] convergent coupling

reaction between disaccharide donor 5 or 6 and trisaccharide acceptor 7, which in turn could be derived from building blocks 8–14 (Scheme 1b). The aminopropyl linker at the reducing end of 1–4 was designed to conjugate the final antigen to a protein to enable immunological studies and analysis.

To construct the  $\alpha$ -glycosidic bond at the reducing end of the target pentasaccharides, we started with the thioglycoside donor



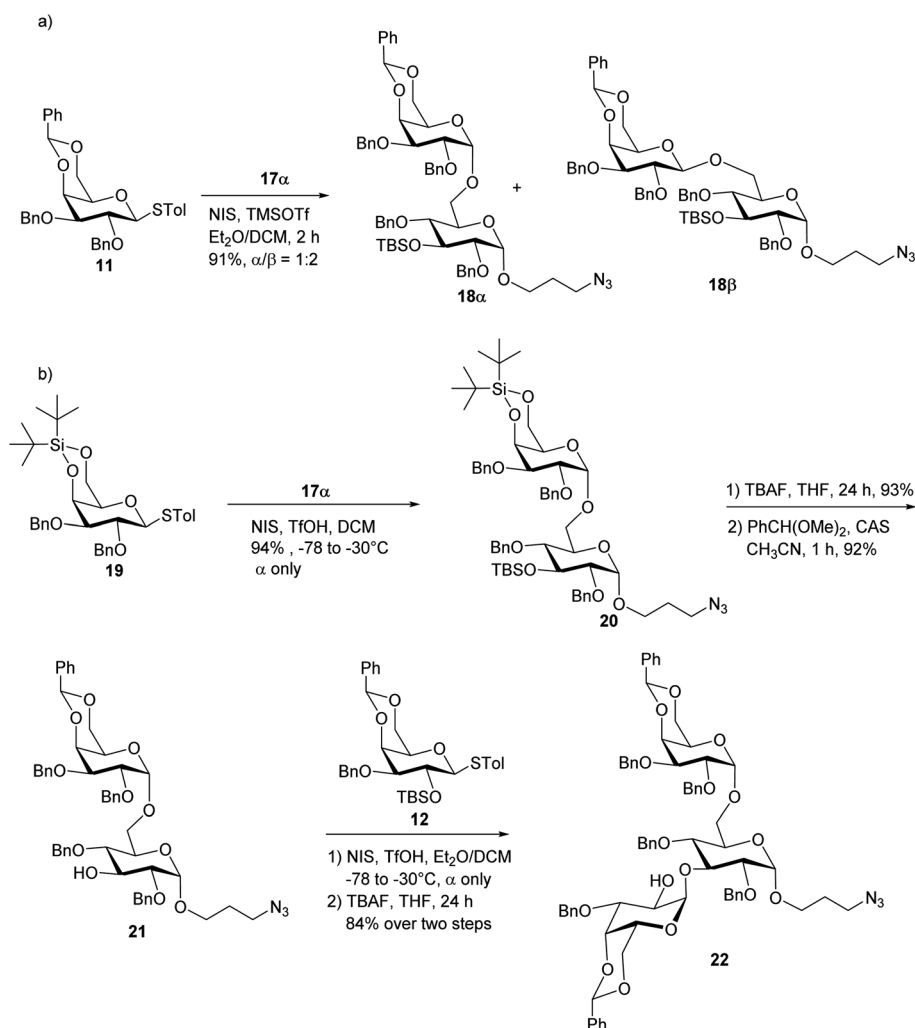
Scheme 2 Syntheses of the non-reducing end monosaccharide acceptors 15 $\alpha$  and 17 $\alpha$ .



**13**,<sup>33</sup> which contains a 6-*O* Bz (benzoyl) group potentially helping to enhance the  $\alpha$ -selectivity.<sup>34</sup> Thioglycoside **13** was treated with 3-amino-1-propanol derivative **14** in the presence of *N*-iodosuccinimide (NIS) and triflic acid (TfOH) as the promoter and diethyl ether (Et<sub>2</sub>O)/dichloromethane (DCM) as the solvent, which resulted in an inseparable anomeric mixture of the products (Scheme 2). Removal of the Bz moiety from the products enabled the isolation of glucosides **15 $\alpha$**  and **15 $\beta$**  in 51% and 34% yields respectively. Interestingly, when the acceptor was changed to 3-azidopropan-1-ol **16** for the glycosylation reaction by donor **13** followed by subsequent treatment with NaOCH<sub>3</sub>, compound **17 $\alpha$**  was produced in 84% yield, along with the  $\beta$ -anomer **17 $\beta$**  as a minor product (8%) (Scheme 2). In compound **17 $\alpha$** , the  $\alpha$ -configuration of the glucopyranosidic linkage was established by its H-1/H-2 coupling constant ( $^3J_{\text{H-1/H-2}} = 3.7$  Hz). The reason for higher  $\alpha$ -stereoselectivity achieved with 3-azidopropan-1-ol **16** is not clear, which may be due to its better matching with the 1,2-*cis* reaction trajectory toward the activated donor.

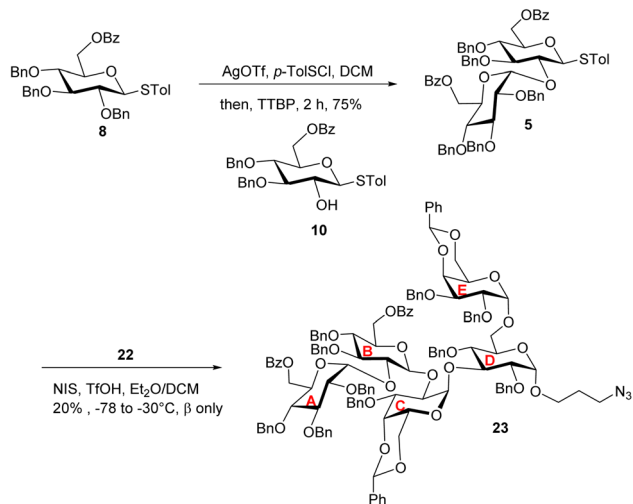
With the reducing end building blocks prepared, glycosylation between compounds **11**<sup>35</sup> and **17 $\alpha$**  was initiated using NIS

and TfOH as the promoter. Although donor **11** lacked a classical participating neighboring group at the 2-*O* position, this reaction led to the  $\beta$ -configured disaccharide **18 $\beta$**  as the major product (Scheme 3a). To achieve the desired  $\alpha$ -linked disaccharide, 4,6-*O*-silylidene protected donor **19**<sup>36</sup> was subsequently explored.<sup>37</sup> Glycosylation of **19** with **17 $\alpha$**  led to compound **20** exclusively as the  $\alpha$ -anomer in 94% yield. The  $\alpha$ -configuration of the new galactopyranosidic linkage in **20** was determined by its H-1/H-2 coupling constant ( $^3J_{\text{H-1/H-2}} = 3.6$  Hz). Transformation of compound **20** into the disaccharide acceptor **21** involved the deprotection of the silylidene and *tert*-butyldimethylsilyl (TBS) groups with tetrabutylammonium fluoride (TBAF), followed by benzylidene protection at galactose's 4-*O* and 6-*O* positions generating disaccharide acceptor **21**. The glycosylation of compound **21** with thiogalactosyl donor **12** proceeded efficiently, affording the desired trisaccharide. Subsequent removal of the TBS protecting group using TBAF furnished trisaccharide acceptor **22** in an overall yield of 84% over two steps. The newly formed galactopyranosidic linkage was confirmed by its characteristic  $^3J_{\text{H-1/H-2}}$  coupling constant of 3.8 Hz (Scheme 3b).



Scheme 3 (a) Syntheses of disaccharide acceptor **18 $\alpha$**  and **18 $\beta$** ; and (b) synthesis of trisaccharide acceptor **22**.





Scheme 4 [2 + 3] glycosylation between disaccharide donor 5 and acceptor 22 gave the pentasaccharide 23 with the undesired  $\beta$ -linkage between B and C units.

To prepare the non-reducing end disaccharide donor, the 6-*O* Bz bearing thioglucosyl donor **8**<sup>38</sup> was pre-activated with *p*-TolSfCl/AgOTf<sup>39</sup> at  $-78$  °C and glycosylated thioglycosyl acceptor **10** producing disaccharide **5** in 75% yield (Scheme 4). The H-1/H-2 coupling constant of the newly formed glucopyranosidic linkage in **5** was 3.8 Hz indicating  $\alpha$ -bond formation. With disaccharide donor **5** and trisaccharide **22** in hand, we proceeded to construct the pentasaccharide framework *via* the [2 + 3] glycosylation reaction (Scheme 4). Unexpectedly, the resulting glycosidic bond had the  $\beta$ -configuration with no  $\alpha$ -glycoside product isolated. The configuration of the newly formed glycosidic linkage was determined by <sup>1</sup>H-coupled gHSQC-NMR, with a coupling constant of <sup>3</sup>*J*<sub>H-1/H-2</sub> at 7.8 Hz and <sup>3</sup>*J*<sub>H-1/C-1</sub> at 164.4 Hz.<sup>40</sup>

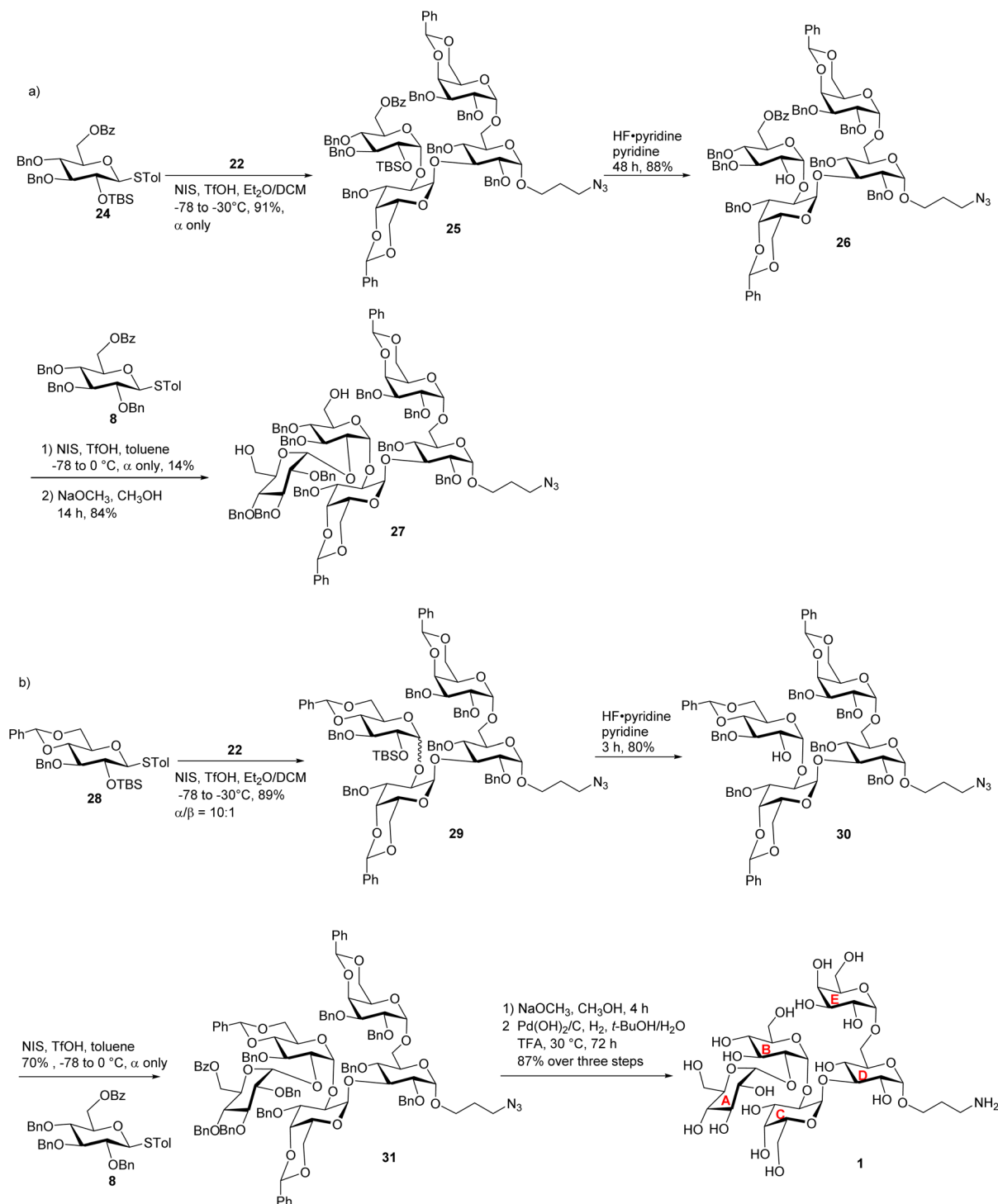
To overcome the stereoselectivity problem in forming the glycosidic linkage between the B and C units in **23**, an alternative stepwise sugar chain extension strategy was investigated. The 2-*O*-TBS protected glucoside donor **24** underwent glycosylation with the trisaccharide acceptor **22** in the presence of NIS and TfOH with DCM and Et<sub>2</sub>O as solvents, yielding tetrasaccharide **25** (Scheme 5a). Unlike in the synthesis of pentasaccharide **23**, the newly formed glucopyranosidic linkage in **25** has a <sup>3</sup>*J*<sub>H-1/H-2</sub> of 3.2 Hz supporting the  $\alpha$  linkage. The divergent stereochemical outcome with disaccharide donor **5** vs. monosaccharide **24** was presumably due to the higher steric hindrance posed by the glycan ring at the 2-*O* position of **5**, which precluded the nucleophilic attack by the acceptor from the  $\alpha$  face. Deprotection of the TBS group from tetrasaccharide **25** by HF·pyridine afforded tetrasaccharide acceptor **26** with a yield of 88%. This reaction progressed slowly requiring 48 hours for completion. Acceptor **26** was glycosylated with monosaccharide donor **8** in toluene at room temperature for 2 hours, affording the glycoside product in 14% yield. It is noteworthy that when DCM was used as the solvent, no desired product was isolated. Subsequent Bz deprotection gave exclusively pentasaccharide **27** with the  $\alpha$ -configuration in 84% yield.

To better understand the low yield in the formation of **27**, we performed conformational analysis of compound **26**. Density Functional Theory (DFT) calculation indicated that in compound **26**, its free hydroxyl group (OH) is well shielded by neighboring groups (Fig. S2†), thus presenting low nucleophilicities. To reduce the steric hindrance, we designed the 4,6-*O* benzylidene protected glucosyl acceptor **28** (Scheme 5b). Computational analysis showed that in the corresponding tetrasaccharide (compound **30**), its free OH group is more accessible (Fig. S2a†), which should enhance the glycosylation yield. To test this hypothesis, we started with the glycosylation of trisaccharide acceptor **22** by monosaccharide donor **28** under NIS and TfOH condition, which led to an  $\alpha/\beta$  ratio of 10 : 1 of tetrasaccharide **29** in 89% yield (Scheme 5b). The subsequent TBS deprotection of this mixture was completed within 2 hours, which was significantly faster than the TBS deprotection from **25** supporting the reduced steric hindrance around the 2-*O*-TBS moiety in **29**. Following TBS deprotection, the  $\alpha$  and  $\beta$  isomers were separated using silica gel column chromatography yielding the pure  $\alpha$  anomer **30** in 80% yield. In compound **30**, the newly formed glucosidic bond had a chemical shift at 4.92 ppm with a coupling constant of <sup>3</sup>*J*<sub>H-1/H-2</sub> of 3.9 Hz. The modified tetrasaccharide acceptor **30** was then glycosylated with monosaccharide donor **8**, yielding the pentasaccharide **31** in 70% yield. The change of 4-*O* and 6-*O* benzyl groups in tetrasaccharide **26** to the 4,6-*O* benzylidene protective group in tetrasaccharide acceptor **30** increased the yield of the pentasaccharide product by fivefold.

After achieving the fully protected pentasaccharide framework as **31**, its Bz groups were removed using sodium methoxide, followed by catalytic hydrogenation and azide reduction, ultimately yielding the target product **1** with an overall yield of 87% in two steps (Scheme 5b). The structure of compound **1** was confirmed by NMR and high-resolution mass spectrometry (HRMS) analyses. All glycosidic bond configurations in **1** were verified based on NMR data (<sup>3</sup>*J*<sub>H-1/H-2</sub> coupling constants): <sup>3</sup>*J*<sub>H-1/H-2</sub> of 3.5 Hz corresponds to unit A  $\alpha$ -GlcP linkage; <sup>3</sup>*J*<sub>H-1/H-2</sub> of 3.8 Hz corresponds to unit B  $\alpha$ -GlcP linkage; the <sup>3</sup>*J*<sub>H-1/H-2</sub> of unit C  $\alpha$ -GalP linkage is 3.8 Hz; <sup>3</sup>*J*<sub>H-1/H-2</sub> of 3.8 Hz corresponds to unit D  $\alpha$ -GlcP; and the <sup>3</sup>*J*<sub>H-1/H-2</sub> of 2.2 Hz is associated with unit E  $\alpha$ -GalP. Further support for the structure came from the HRMS data, which provided an (M + H)<sup>+</sup> signal at *m/z* 886.3397 (calcd 886.3397). In addition, ROESY-NMR analysis was performed on pentasaccharide **1**. Correlations were observed between the anomeric protons of the three monosaccharide units from the non-reducing end (Fig. S2b†), suggesting that these three residues were close to each other in space confirming the sterically congested nature of pentasaccharide **1**.

Pentasaccharides **1** and **2** share similar structural features, enabling the synthesis strategy developed for compound **1** to be adapted to compound **2**. For compound **2**, as its non-reducing end unit (unit A) is 1,2-*cis* linked *N*-acetyl (NHAc) glucosamine, donor **9** bearing a 2-N<sub>3</sub> moiety was selected to form the non-reducing end linkage between units A and B. To avoid the need to differentiate multiple azido groups, **15** $\alpha$  was utilized as the reducing end building block. **15** $\alpha$  was glycosylated by galactose donor **19** producing compound **32** in 94% yield



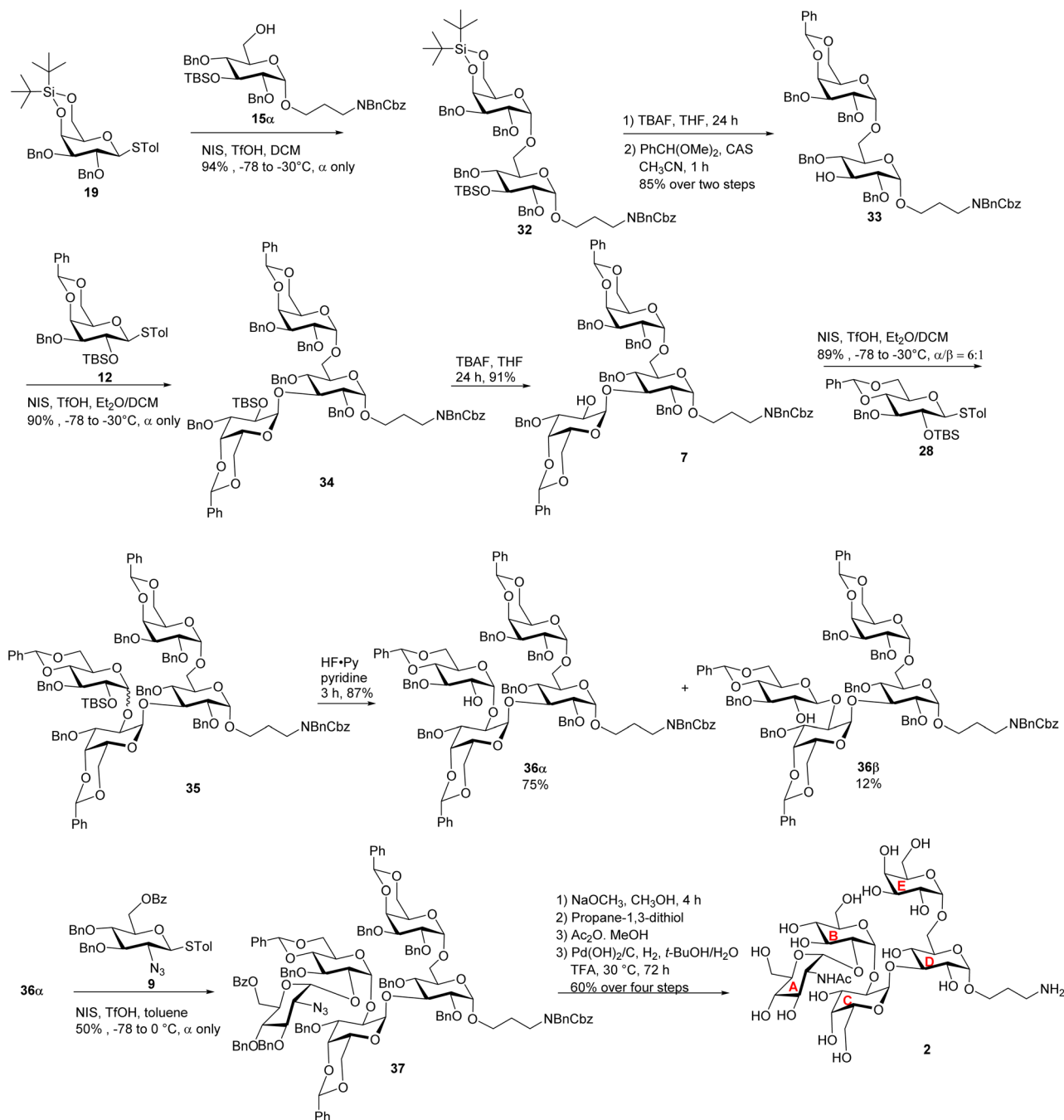


Scheme 5 (a) Synthesis of the fully protected pentasaccharide 27; and (b) synthesis of target pentasaccharide 1.

(Scheme 6). The newly formed galactopyranosyl linkage was determined to be  $\alpha$  as it displayed a coupling constant ( $^3J_{\text{H-1/H-2}}$ ) of 3.5 Hz. Compound 32 was then converted into 33 through TBS and silylidene deprotection, followed by benzylidene protection at the 4,6-O positions of the galactose residue. With disaccharide 33 in hand, glycosylation was performed between

33 and 12 resulting in compound 34, which was subsequently deprotected to yield acceptor 7. Under NIS/TfOH promotion, 28 reacted with compound 7, generating an  $\alpha/\beta$  mixture of glycosides ( $\alpha/\beta = 6:1$ , compound 35). The TBS group of 35 was removed using HF-pyridine, and after purification by flash column chromatography, the resulting compounds 36 $\alpha$  and





Scheme 6 Synthesis of the target pentasaccharide 2.

36 $\beta$  were obtained in 75% and 12% yields, respectively. Using acceptor 36 $\alpha$ , the final glycosidic bond was then formed with donor 9,<sup>41</sup> leading to compound 37 with exclusive  $\alpha$ -selectivity and a 50% yield. The coupling constants of the five  $\alpha$ -glycosidic bonds were confirmed by the  $^1\text{H}$ - $^{13}\text{C}$  decoupled gHSQC spectrum to be  $J = 171.9$  Hz, 169.8 Hz, 171.7 Hz, 171.9 Hz, and 169.6 Hz. Global deprotection of compound 37 was achieved through three steps: (1) removal of the Bz group with  $\text{NaOCH}_3$ , (2) reduction of the azido group to an amine using propane-1,3-dithiol, followed by acetylation of the free amine, and (3)

catalytic hydrogenation over  $\text{Pd(OH)}_2/\text{C}$  to remove all remaining protecting groups. After purification through size exclusion chromatography, the deprotected pentasaccharide was obtained as a white solid, yielding 2 in 60% over four steps. The glycosidic bond configurations in 2 were confirmed by NMR data ( $^3J_{\text{H-1/H-2}}$  coupling constants): the  $^3J_{\text{H-1/H-2}}$  of the unit A  $\alpha$ -Glc $\beta$  linkage is 3.7 Hz; the  $^3J_{\text{H-1/H-2}}$  of the unit B  $\alpha$ -Glc $\beta$  is 3.7 Hz; the  $^3J_{\text{H-1/H-2}}$  of the unit C  $\alpha$ -Gal $\beta$  linkage is 3.6 Hz; the  $^3J_{\text{H-1/H-2}}$  of unit D  $\alpha$ -Glc $\beta$  is 3.9 Hz, and the  $^3J_{\text{H-1/H-2}}$  of the unit E  $\alpha$ -Gal $\beta$  linkage is 3.7 Hz. Further confirmation of the structure came

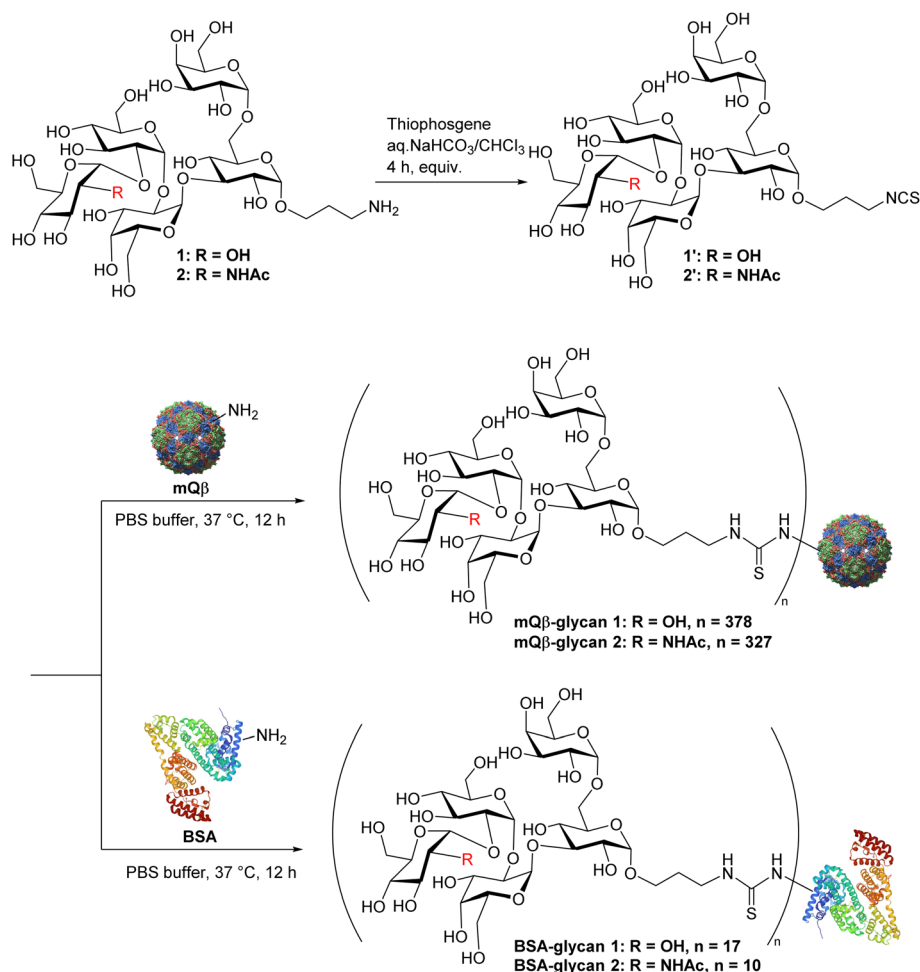


from HRMS data, showing an  $(M + H)^+$  signal at  $m/z$  927.3633 (calcd 927.3669). In parallel to the syntheses of pentasaccharides **1** and **2**, outer core tetrasaccharide **3** and disaccharide **4** were synthesized (Scheme S8†).

### Bioconjugation of *Salmonella* LPS outer core glycans to enable vaccine studies

Carbohydrate antigens are generally T cell-independent B cell antigens, resulting in weak immunogenicity when administered alone. Conjugation with an appropriate carrier is a well-established strategy to enhance the anti-carbohydrate antibody

responses.<sup>42,43</sup> The mutant bacteriophage Q $\beta$  (mQ $\beta$ ) has shown considerable potential as a carrier for carbohydrate-based conjugate vaccines.<sup>44–46</sup> To enable efficient bio-conjugation of antigens **1** and **2** with mQ $\beta$ , an isothiocyanate (NCS) group was introduced at the N-terminus of each antigen, producing pentasaccharides **1'** and **2'**, which were incubated overnight with mQ $\beta$  (6 equiv. per amine) (Scheme 7). LC-MS analysis indicated that an average of 378 copies of **1** and 327 copies of **2** were loaded onto each mQ $\beta$  particle respectively. To measure anti-glycan responses while minimizing interference from anti-mQ $\beta$  antibodies, bovine serum albumin (BSA)-glycan **1**



Scheme 7 Conjugation of glycans with mQ $\beta$  and BSA.

Table 1 Experimental mouse groups and immunization parameters

Group	Vaccine construct	Glycan per dose ( $\mu$ g)	Adjuvant	Immunization schedule (days)
A	mQ $\beta$ -glycan <b>1</b>	5	Alum	0, 14, 28
B	mQ $\beta$ -glycan <b>2</b>	5	Alum	0, 14, 28
C	mQ $\beta$ -glycan <b>2</b>	1	Alum	0, 14, 28
D	mQ $\beta$ -glycan <b>2</b>	1	—	0, 14, 28
E	mQ $\beta$ , glycan <b>1</b> , glycan <b>2</b> admixture	5	Alum	0, 14, 28



and 2 conjugates were synthesized (Scheme 7) and used as the coating antigen in ELISA analyses. In addition, BSA conjugates with glycans 3 and 4 were synthesized for epitope mapping, bearing an average of 13 and 20 glycan moieties per BSA molecule, respectively, as quantified by MALDI-MS (Fig. S3†).

### Both mQ $\beta$ -glycan 1 and mQ $\beta$ -glycan 2 induced high antibody responses in mice and rabbits

The immunogenicity of mQ $\beta$ -glycan 1 and mQ $\beta$ -glycan 2 constructs was evaluated in female C57BL/6 mice ( $n = 5$  per group) through a three-dose subcutaneous immunization schedule on days 0, 14, and 28 at 1  $\mu$ g or 5  $\mu$ g of glycan antigen per dose with or without aluminum hydroxide (Alum) adjuvant (Table 1). Thirty-five days post-initial immunization, mouse serum antibody titers were assessed by enzyme-linked

immunosorbent assay (ELISA). Group A, immunized with mQ $\beta$ -glycan 1 (5  $\mu$ g of glycan 1 per dose), demonstrated high anti-glycan 1 IgG titers, averaging  $2.4 \times 10^6$  ELISA units (Fig. 2a). Similarly, Group B, receiving mQ $\beta$ -glycan 2 (5  $\mu$ g of glycan 2 per dose), achieved a high geometric mean anti-glycan 2 IgG titer of  $6.2 \times 10^5$  ELISA units (Fig. 2b). In contrast, group C with 1  $\mu$ g of glycan 2 per dose showed inconsistent responses, with significant variability across mice and a geometric mean anti-glycan 2 IgG titer of  $1.6 \times 10^4$  ELISA units (Fig. 2b). Group D (mQ $\beta$ -glycan 2, 1  $\mu$ g of glycan 2 per dose, no Alum adjuvant) and group E (admixture of mQ $\beta$  with 5  $\mu$ g of glycans 1 and 2 each) exhibited low anti-glycan IgG titers below 1000 ELISA units (Fig. 2a and b), which were similar to the pre-vaccination (Pre) levels. These findings suggest that adjuvant inclusion is essential for eliciting robust antibody responses at the 1  $\mu$ g dose, and more consistent

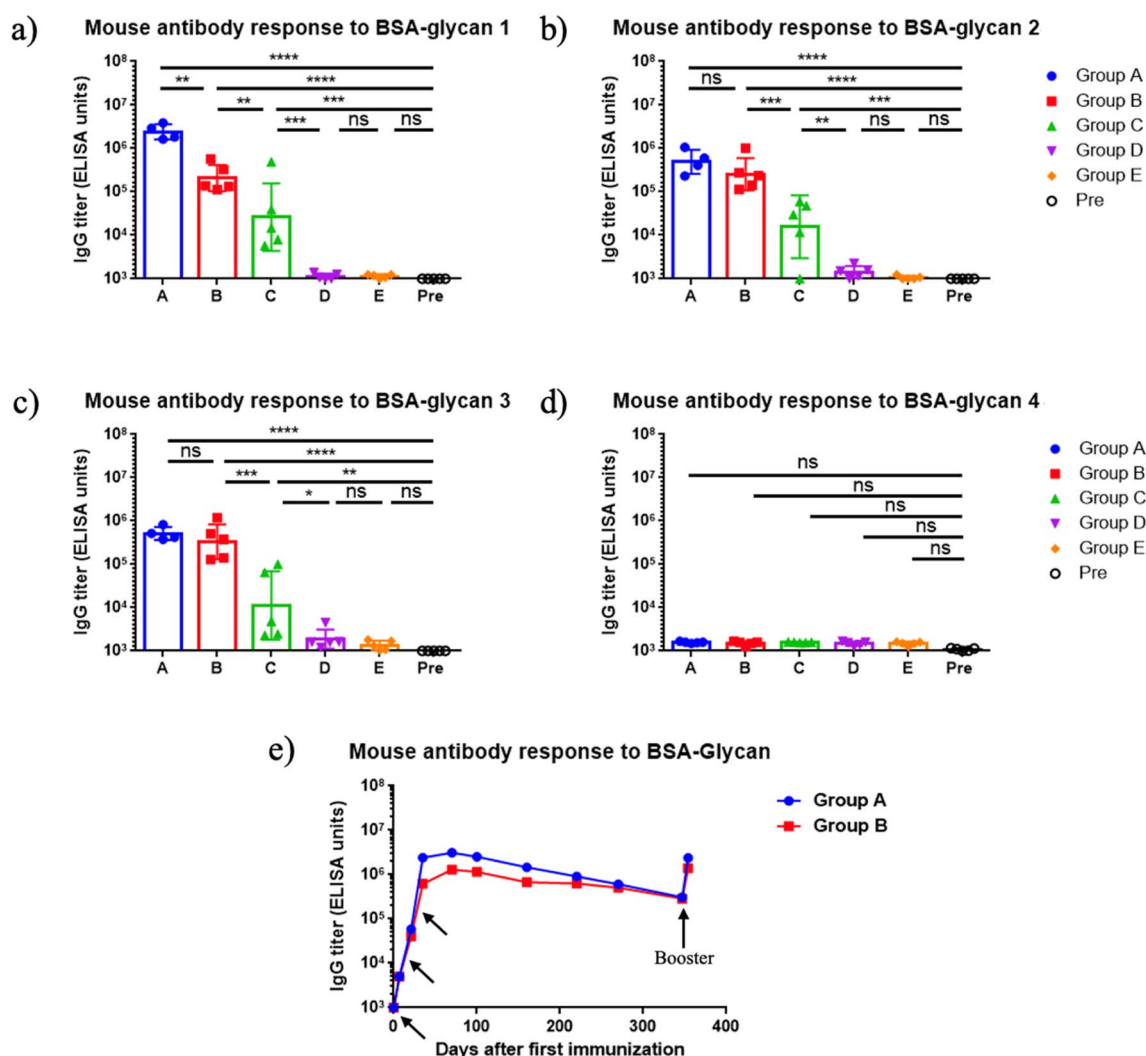


Fig. 2 (a–d) Endpoint values of serum IgG titers at day 35 after immunization against various oligosaccharides. Groups A–E refer to the groups in Table 1. Pre: pre-immunization mouse sera. The endpoint value represents the reciprocal of the last serum dilution that yields an absorbance value three times the standard deviation above the plate blank. Each symbol corresponds to an individual animal. Data are presented as geometric mean values  $\pm$  standard deviation. Statistical significance was determined using one-way ANOVA followed by Tukey's multiple comparisons test. ns:  $p > 0.05$ ; \*:  $p \leq 0.05$ ; \*\*:  $p \leq 0.01$ ; \*\*\*:  $p \leq 0.001$ ; \*\*\*\*:  $p \leq 0.0001$ . (e) Persistence of antibody responses. Each symbol represents pooled sera from group A (measured against BSA-glycan 1) or group B (measured against BSA-glycan 2) at various time points. Arrows indicate the days of vaccination (days 0, 14, 28, 360).



immune responses were induced with 5  $\mu\text{g}$  of antigen. In addition, it is critical to covalently conjugate the mQ $\beta$  carrier with the antigen.

To profile the epitope specificity of antibodies induced by mQ $\beta$ -glycan 1 and mQ $\beta$ -glycan 2, cross-recognition of the two pentasaccharides was examined using sera collected on day 35 post-primary immunization (Fig. 2a and b), and the binding of the post-immunization sera with BSA conjugates of tetrasaccharide 3 and disaccharide 4 was also analyzed (Fig. 2c and d). Group A (immunized with mQ $\beta$ -glycan 1) exhibited high levels of anti-glycan 2 IgG antibodies, with a geometric mean IgG titer of  $5 \times 10^5$  ELISA units (Fig. 2b). Conversely, Group B (immunized with mQ $\beta$ -glycan 2) demonstrated an average anti-glycan 1 IgG titer of  $2 \times 10^5$  ELISA units. The ELISA titers against tetrasaccharide 3 were measured as  $5.1 \times 10^5$  ELISA units for group A and  $3.3 \times 10^5$  ELISA units for group B, suggesting Glc and GlcNHAc at the non-reducing ends of pentasaccharides 1 and 2 did not significantly influence antigen binding. No binding was detected for disaccharide 4, indicating that the reducing end disaccharide is not a major epitope for mouse antibody recognition.

For an effective vaccine, the ability to generate long-term immune responses is highly desired. Monitoring the serum IgG titers over more than 360 days demonstrated that the antibody responses induced by mQ $\beta$ -glycan 1 and mQ $\beta$ -glycan 2 were durable. As shown in Fig. 2e, average IgG titers in mice immunized with mQ $\beta$ -glycan 1 and mQ $\beta$ -glycan 2 peaked on day 56, reaching  $3.1 \times 10^6$  and  $1.3 \times 10^6$  ELISA units, respectively. Strong IgG responses were maintained with average IgG titers of  $3.1 \times 10^5$  and  $2.9 \times 10^5$  ELISA units on day 360. Following a booster on day 360, antibody titers returned to near peak values, suggesting that vaccine-induced immune memory was generated and could be effectively recalled even after a prolonged period. In contrast, Groups D and E showed low anti-glycan titers ( $<10^3$  ELISA units) throughout the study. These results suggest that mQ $\beta$ -glycan 1 and mQ $\beta$ -glycan 2, when administered with Alum, elicit robust, long-lasting antibody response and durable immunity.

To evaluate immunogenicity across multiple species and aid in future translation, rabbits were immunized subcutaneously with mQ $\beta$ -glycan 1 and mQ $\beta$ -glycan 2. Four groups of rabbits received various vaccines as outlined in Table 2. Injections were

Table 2 Experimental rabbit groups and immunization details

Group	Vaccine construct	Glycan per dose ( $\mu\text{g}$ )	Adjuvant	Immunization schedule (days)
F	mQ $\beta$ -glycan 1	5	Alum	0, 14, 28, 42
G	mQ $\beta$ -glycan 1	15	Alum	0, 14, 28, 42
H	mQ $\beta$ -glycan 2	5	Alum	0, 14, 28, 42
I	mQ $\beta$ -glycan 2	5	MPLA	0, 14, 28, 42

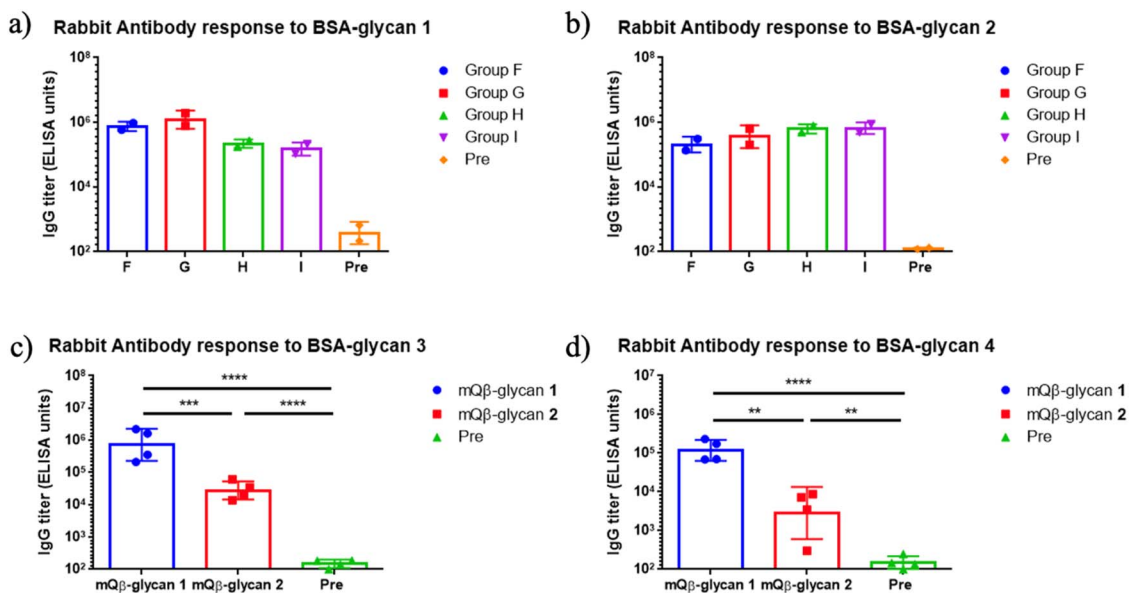


Fig. 3 (a–d) Endpoint values of IgG titers against various oligosaccharides. The endpoint value represents the reciprocal of the last serum dilution that yields a signal three times the standard deviation above the plate blank. Each symbol corresponds to an individual animal. Data are presented as geometric mean values  $\pm$  standard deviation. Statistical significance was determined using one-way ANOVA followed by Tukey's multiple comparisons test. \*\*:  $p \leq 0.01$ ; \*\*\*:  $p \leq 0.001$ ; \*\*\*\*:  $p \leq 0.0001$ . Pre: pre-immunization rabbit sera.



administered on days 0, 14, 28, and 42, with the final blood sample collected on day 49. ELISA analysis of post-immune sera demonstrated robust anti-glycan IgG responses in all four groups with endpoint titers exceeding  $10^5$  ELISA units (Fig. 3a and b), while the anti-glycan IgG titers in pre-immune sera were around 200 ELISA units. No adverse effects from the vaccinations were observed in either rabbits or mice.

To further assess antibody specificity, BSA conjugates of glycan 3 and glycan 4 were used as coating antigens in ELISA. Post-immune rabbit sera showed a marked increase in binding to glycan 3 compared to pre-immune sera, similar to results observed in mice (Fig. 3c). However, unlike mouse sera, post-immune rabbit sera exhibited a significant increase in binding to glycan 4 (Fig. 3d). These results suggest that, even

with the same antigenic construct, the epitope profiles recognized by antibodies can differ across animal species.

Next, we analyzed vaccine-induced IgG antibody binding to the native polysaccharide (*i.e.*, core and O-polysaccharide (COPS)) isolated from four *Salmonella* strains. The rabbit sera on day 49 post-vaccination exhibited significantly enhanced binding (by 10- to 50-fold) to COPS compared to pre-immunization levels (see ESI Fig. S5†). In contrast, mouse serum showed no recognition of native COPS. Similar species-specific differences in immune responses were also observed in previous studies.<sup>21,22</sup> This may be due to the rabbit's distinct evolutionary lineage, limited inbreeding, and unique immune repertoire development, which together enable rabbits to

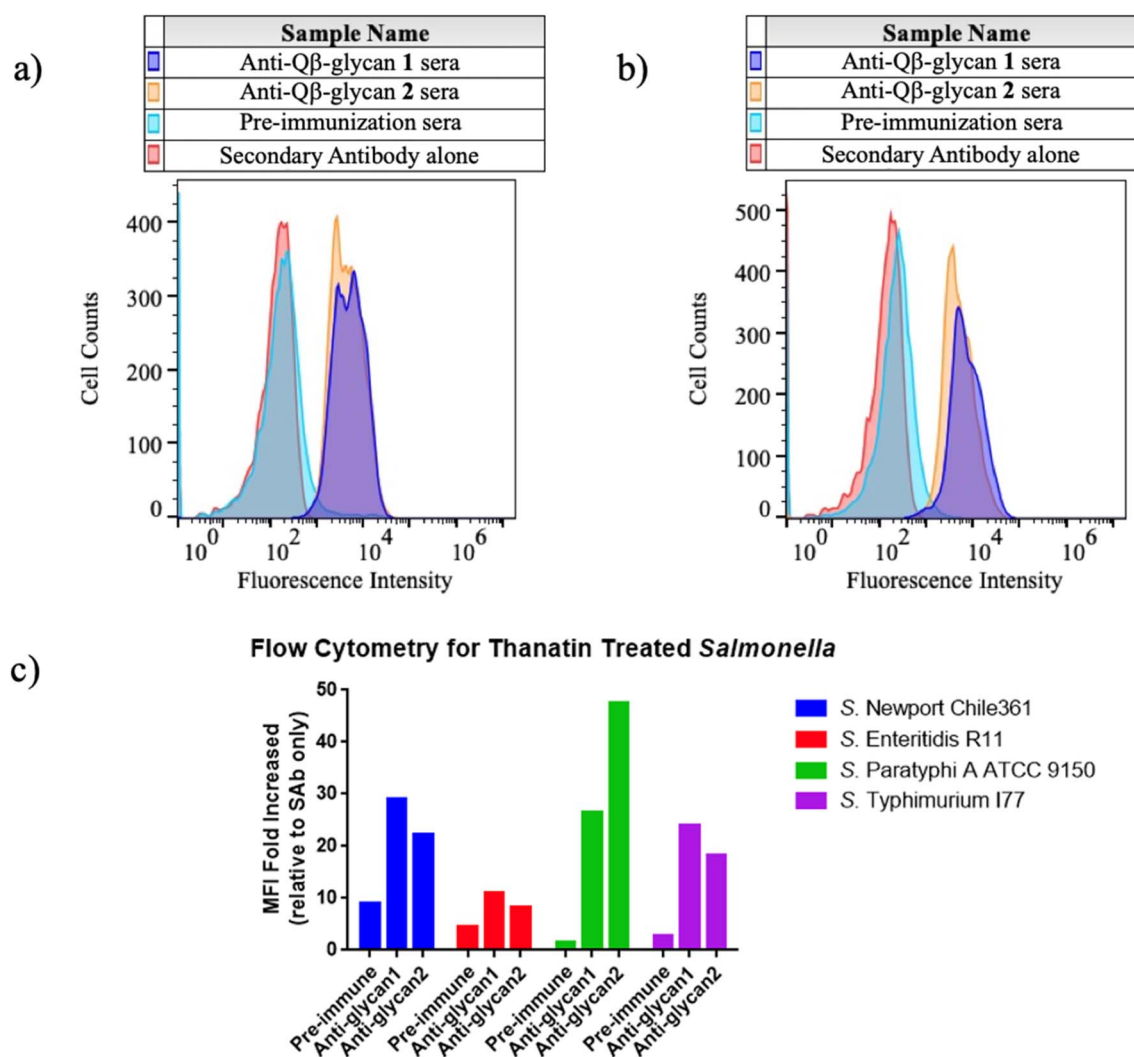


Fig. 4 mQ $\beta$ -glycan 1 and mQ $\beta$ -glycan 2 induced rabbit antibodies bind *Salmonella* rough strains. (a) Flow cytometry graphs of post-immunization sera (1 : 100 dilution) binding with the *S. Enteritidis* R11  $\Delta invA \Delta rfaL$  strain, as compared to the anti-rabbit IgG secondary antibody alone or pre-immunization rabbit sera (1 : 100 dilution). (b) Flow cytometry graphs of post-immunization sera (1 : 100 dilution) binding with the *S. Newport*  $\Delta rfaL$  strain, as compared to the anti-rabbit IgG secondary antibody alone or pre-immunization rabbit sera (1 : 100 dilution). (c) Mean fluorescence intensity (MFI) flow cytometry graphs of pre-immunization rabbit sera (1 : 50 dilution) and post-immunization sera (1 : 50 dilution) binding with thanatin-treated *S. Enteritidis* R11, *S. Typhimurium* I77, *S. Newport* Chile 361, *S. Paratyphi* A ATCC 9150. The results were compared to the fold increase relative to the FTIC-conjugated anti-rabbit IgG secondary antibody alone group. Secondary alone refers to cells treated with secondary antibodies only without any sera.



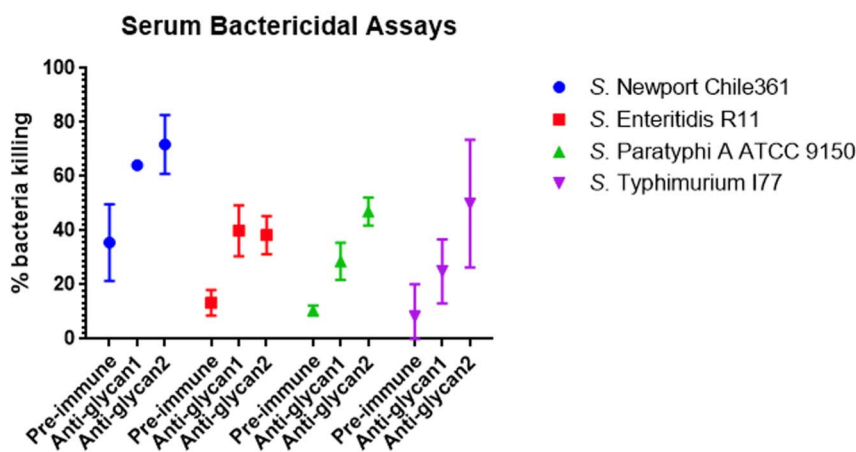


Fig. 5 Rabbit anti-mQ $\beta$ -glycan 1 or anti-mQ $\beta$ -glycan 2 pooled sera ( $n = 2$  per group) enhanced complement-mediated *Salmonella* killing. Log-phase cultures of *Salmonella* were incubated with thanatin, opsonized with heat-inactivated rabbit sera, followed by the addition of baby rabbit complement to eliminate opsonized *Salmonella*. Viable bacterial counts, expressed as colony-forming units (CFUs), were determined through serial dilution and plating.

mount broader and more sensitive antibody responses than rodents.<sup>47</sup>

#### Immunization with mQ $\beta$ -glycan 1 and mQ $\beta$ -glycan 2 elicited high titers of anti-glycan IgG antibodies capable of binding *Salmonella* belonging to different serogroups

The binding capacity of rabbit antisera to live *Salmonella* bacteria was assessed next by flow cytometry. As shown in Fig. 4, minimal binding to *Salmonella* rough strains (which lack long-chain OPS but express the core oligosaccharide) was observed for pre-immunization sera at a 1:100 dilution, compared to samples without sera. In contrast, IgG antibodies induced by either mQ $\beta$ -glycan 1 or mQ $\beta$ -glycan 2 in rabbits showed strong binding to rough strains: *S. Enteritidis* R11  $\Delta invA \Delta rfaL$  (Fig. 4a, ESI Fig. S6<sup>†</sup>) and *S. Newport* Chile 361  $\Delta rfaL$  (Fig. 4b, ESI Fig. S6<sup>†</sup>). In contrast, all sera exhibited slight binding to smooth *Salmonella* strains, including *S. Enteritidis* R11, *S. Typhimurium* I77, *S. Newport* Chile 361 and *S. Paratyphi* A ATCC 9150, which share an outer core structure identical to glycan 1. This indicates that the high density of OPS possibly conceals the core oligosaccharide, preventing antibody access and binding in our experiments.

As a major difference between the smooth and rough strains of *Salmonella* is that smooth strains express long LPS on the surface; we hypothesized that reducing the LPS density on the bacteria may enhance the access and the binding of the core LPS by antibodies. To test this, the four smooth *Salmonella* strains were treated with 0.5  $\mu\text{M}$  thanatin (50% of the minimum inhibitory concentration for Gram-negative bacteria), an inhibitor of LPS transport proteins LptA and LptD.<sup>48</sup> After thanatin treatment, post-immunization sera showed significantly increased binding compared to pre-immunization sera (Fig. 4c), with no notable difference observed between anti-glycan 1 and anti-glycan 2 rabbit sera. These results suggest that treatment

with thanatin significantly improved access to the outer core by antibodies.

With enhanced binding following LPS transport inhibition, a serum bactericidal activity assay was conducted to evaluate antibody-dependent, complement-mediated killing. *Salmonella* cells were incubated with thanatin, grown to the logarithmic phase ( $\text{OD} = 0.4$ ), opsonized with sera (diluted by 50-fold) at 4 °C overnight, and incubated with baby rabbit complement at 37 °C for one hour. Anti-glycan sera significantly enhanced the killing of all four *Salmonella* strains compared to pre-immune sera (Fig. 5).

## Conclusions

Oligosaccharides 1–4 associated with *Salmonella* common outer core oligosaccharides have been synthesized using concise synthetic strategies, marking the first successful syntheses of these sequences. The stereoselective formation of all five 1,2-*cis* glycosidic linkages was assisted by judicious choice of protective groups and matching the donor and the acceptor structures. The low yield observed in the key glycosylation steps of compounds 8 and 26 was attributed to steric hindrance around the free OH in acceptor 26 as deciphered by computational studies. Following synthesis, the two outer core pentasaccharides 1 and 2 were successfully conjugated to a powerful immunogenic carrier, bacteriophage mQ $\beta$ . Parenteral immunization with these conjugates effectively induced potent serum IgG antibody responses in both mice and rabbits. Antibodies produced in immunized rabbits were able to recognize multiple rough strains of *Salmonella*. For the major pathogenic smooth *Salmonella* strains tested, the addition of an LPS transport protein inhibitor thanatin facilitated effective bacterial binding with antiserum. The improved binding of thanatin-treated bacteria to the antiserum was accompanied by significantly more efficient serum bactericidal activities with both anti-



glycan 1 and anti-glycan 2 sera compared to pre-immune sera. The induction of a robust antibody response against the LPS core through vaccination followed by treatment with a low concentration of thanatin, an LPS transport inhibitor upon infection, represents a new strategy for further investigation.<sup>49</sup>

## Experimental section

Detailed experimental procedures are provided in the ESI.†

## Ethical statement

All animal procedures were performed in accordance with the Guidelines for Care and Use of Laboratory Animals of Michigan State University and approved by the Institutional Animal Care and Use Committee (IACUC) of Michigan State University (protocol number: 202200444).

## Data availability

The data supporting this article have been included as part of the ESI.†

## Author contributions

X. H. and X. P. conceived and designed the project. X. P. performed the experimental work. F. S. assisted with mouse cardiac puncture. X. P. and T.-A. C. conducted the computational studies. X. H. supervised both experimental and computational work. S. M. T. and S. M. B. extracted and provided the *Salmonella* COPS and all *Salmonella* strains used in the study. X. P. and X. H. wrote the manuscript. All authors reviewed and approved the final version of the manuscript.

## Conflicts of interest

Xuefei Huang is the founder of Iaso Therapeutics Inc., which is dedicated to the development of the next generation of vaccines. There are no conflicts to declare for other authors.

## Acknowledgements

We are grateful for financial support from the National Institute of Allergy and Infectious Diseases, NIH (R01AI146210, R01AI182419 (XH), K01AI168587 (SMB)) and Michigan State University for financial support of our work. We extend our gratitude to Dr Daniel Holmes for help in NMR experiments, and Dr Anthony Schillmiller for insightful discussions regarding HRMS analyses.

## References

- 1 Y. T. Hung, C. J. Lay, C. L. Wang and M. Koo, *J. Infect. Public Health*, 2017, **10**, 518–521.
- 2 A. Galan-Relano, A. Valero Diaz, B. Huerta Lorenzo, L. Gomez-Gascon, M. F. Mena Rodriguez, E. Carrasco

- Jimenez, F. Perez Rodriguez and R. J. Astorga Marquez, *Animals*, 2023, **13**, 3666–3688.
- 3 A. Chlebicz and K. Slizewska, *Int. J. Environ. Res. Public Health*, 2018, **15**, 863–892.
- 4 G. D. D. Collaborators, *Lancet Infect. Dis.*, 2017, **17**, 909–948.
- 5 S. Hoffmann, A. E. White, R. B. McQueen, J. W. Ahn, L. B. Gunn-Sandell and E. J. Scallan Walter, *Foodborne Pathog. Dis.*, 2024, **21**, DOI: [10.1089/fpd.2023.0157](https://doi.org/10.1089/fpd.2023.0157).
- 6 A. J. Browne, B. H. Kashef Hamadani, E. A. P. Kumaran, P. Rao, J. Longbottom, E. Harriss, C. E. Moore, S. Dunachie, B. Basnyat, S. Baker, A. D. Lopez, N. P. J. Day, S. I. Hay and C. Dolecek, *BMC Med.*, 2020, **18**, 1.
- 7 B. E. Karp, H. Tate, J. R. Plumblee, U. Dessai, J. M. Whichard, E. L. Thacker, K. R. Hale, W. Wilson, C. R. Friedman, P. M. Griffin and P. F. McDermott, *Foodborne Pathog. Dis.*, 2017, **14**, 545–557.
- 8 M. A. Gordon, S. M. Graham, A. L. Walsh, L. Wilson, A. Phiri, E. Molyneux, E. E. Zijlstra, R. S. Heyderman, C. A. Hart and M. E. Molyneux, *Clin. Infect. Dis.*, 2008, **46**, 963–969.
- 9 D. R. Bhatta, A. Bangtrakulnonth, P. Tishyadhigama, S. D. Saroj, J. R. Bandekar, R. S. Hendriksen and B. P. Kapadnis, *Lett. Appl. Microbiol.*, 2007, **44**, 588–594.
- 10 K. A. Date, A. E. Newton, F. Medalla, A. Blackstock, L. Richardson, A. McCullough, E. D. Mintz and B. E. Mahon, *Clin. Infect. Dis.*, 2016, **63**, 322–329.
- 11 <https://www.cdc.gov/antimicrobial-resistance/media/pdfs/2019-ar-threats-report-508.pdf>, accessed May 15, 2025.
- 12 E. A. Engels, M. E. Falagas, J. Lau and M. L. Bennish, *BMJ*, 1998, **316**, 110–116.
- 13 A. Fraser, M. Paul, E. Goldberg, C. J. Acosta and L. Leibovici, *Vaccine*, 2007, **25**, 7848–7857.
- 14 M. I. Khan, R. L. Ochiai and J. D. Clemens, *Expert Rev. Vaccines*, 2010, **9**, 485–496.
- 15 V. K. Mohan, V. Varanasi, A. Singh, M. F. Pasetti, M. M. Levine, R. Venkatesan and K. M. Ella, *Clin. Infect. Dis.*, 2015, **61**, 393–402.
- 16 Z. A. Bhutta, M. R. Capeding, A. Bavdekar, E. Marchetti, S. Ariff, S. B. Soofi, A. Anemona, M. A. Habib, E. Alberto, S. Juvekar, R. M. Khan, R. Marhaba, N. Ali, N. Malubay, A. Kawade, A. Saul, L. B. Martin and A. Podda, *Lancet Infect. Dis.*, 2014, **14**, 119–129.
- 17 C. A. MacLennan, J. Stanaway, S. Grow, K. Vannice and A. D. Steele, *Open Forum Infect. Dis.*, 2023, **10**, S58–S66.
- 18 R. Simon and M. M. Levine, *Hum. Vaccines Immunother.*, 2012, **8**, 494–498.
- 19 P. Li, Q. Liu, H. Luo, K. Liang, J. Yi, Y. Luo, Y. Hu, Y. Han and Q. Kong, *Front. Immunol.*, 2017, **8**, 1647–1661.
- 20 C. A. MacLennan, L. B. Martin and F. Micoli, *Hum. Vaccines Immunother.*, 2014, **10**, 1478–1493.
- 21 C. X. Huo, D. Dhara, S. M. Baliban, S. Tahmasebi Nick, Z. Tan, R. Simon, A. K. Misra and X. Huang, *Chem. Commun.*, 2019, **55**, 4519–4522.
- 22 D. Dhara, S. M. Baliban, C. X. Huo, Z. Rashidjahanabad, K. T. Sears, S. T. Nick, A. K. Misra, S. M. Tennant and X. Huang, *Chem.-Eur. J.*, 2020, **26**, 15953–15968.
- 23 A. S. Cross, *Microbiol. Mol. Biol. Rev.*, 2023, **87**, e0004522.



- 24 D. H. Schmiel, E. E. Moran, P. B. Keiser, B. L. Brandt and W. D. Zollinger, *Infect. Immun.*, 2011, **79**, 4146–4156.
- 25 D. Cohen, S. Ashkenazi, M. S. Green, M. Gdalevich, G. Robin, R. Slepion, M. Yavzori, N. Orr, C. Block, I. Ashkenazi, J. Shemer, D. N. Taylor, T. L. Hale, J. C. Sadoff, D. Pavliakova, R. Schneerson and J. B. Robbins, *Lancet*, 1997, **349**, 155–159.
- 26 L. F. Fries, A. D. Montemarano, C. P. Mallett, D. N. Taylor, T. L. Hale and G. H. Lowell, *Infect. Immun.*, 2001, **69**, 4545–4553.
- 27 M. F. Santos, R. R. New, G. R. Andrade, C. Y. Ozaki, O. A. Sant'Anna, L. Mendonca-Previato, L. R. Trabulsi and M. O. Domingos, *Clin. Vaccine Immunol.*, 2010, **17**, 1772–1780.
- 28 N. A. Kaniuk, E. Vinogradov and C. Whitfield, *J. Biol. Chem.*, 2004, **279**, 36470–36480.
- 29 P. A. D. Grimont and F.-X. Weill, in *Antigenic Formulae of the Salmonella Serovars*, Institut Pasteur, Paris, 9th edn, 2007, [https://www.pasteur.fr/sites/default/files/veng\\_0.pdf](https://www.pasteur.fr/sites/default/files/veng_0.pdf).
- 30 S. Muller-Loennies, L. Brade, C. R. MacKenzie, F. E. Di Padova and H. Brade, *J. Biol. Chem.*, 2003, **278**, 25618–25627.
- 31 G. Nagy and T. Pal, *Biol. Chem.*, 2008, **389**, 513–520.
- 32 S. M. Baliban, S. Shridhar, K. Luo, J. Kolasny, S. Hyun, Z. Zhao, S. M. Tennant and A. S. Cross, *J. Infect. Dis.*, 2024, **jiae641**, DOI: [10.1093/infdis/jiae641](https://doi.org/10.1093/infdis/jiae641).
- 33 Q. Zhao, H. Zhang, Y. Zhang, S. Zhou and J. Gao, *Org. Biomol. Chem.*, 2020, **18**, 6549–6557.
- 34 B. S. Komarova, M. V. Orekhova, Y. E. Tsvetkov and N. E. Nifantiev, *Carbohydr. Res.*, 2014, **384**, 70–86.
- 35 Z. Y. Zhang, I. R. Ollmann, X. S. Ye, R. Wischnat, T. Baasov and C. H. Wong, *J. Am. Chem. Soc.*, 1999, **121**, 734–753.
- 36 D. K. Njeri and J. R. Ragains, *Eur. J. Org. Chem.*, 2022, **2022**, e202201261.
- 37 A. Imamura, H. Ando, S. Korogi, G. Tanabe, O. Muraoka, H. Ishida and M. Kiso, *Tetrahedron Lett.*, 2003, **44**, 6725–6728.
- 38 D. Chen, A. K. Srivastava, J. Dubrochowska, L. Liu, T. Li, J. P. Hoffmann, J. K. Kolls and G. J. Boons, *Chem.–Eur. J.*, 2023, **29**, e202203408.
- 39 X. Huang, L. Huang, H. Wang and X. S. Ye, *Angew. Chem., Int. Ed.*, 2004, **43**, 5221–5224.
- 40 K. Bock and C. Pedersen, *J. Chem. Soc., Perkin Trans. 2*, 1974, 293–297.
- 41 Y. Pan, Q. Q. He, N. Wimmer and V. Ferro, *Carbohydr. Res.*, 2024, **545**, 109270.
- 42 Z. Guo and Q. Wang, *Curr. Opin. Chem. Biol.*, 2009, **13**, 608–617.
- 43 Z. Yin and X. Huang, *J. Carbohydr. Chem.*, 2012, **31**, 143–186.
- 44 Z. Rashidjahanabad, S. Ramadan, N. A. O'Brien, A. Nakisa, S. Lang, H. Crawford, J. C. Gildersleeve and X. Huang, *Angew. Chem., Int. Ed.*, 2023, **62**, e202309744.
- 45 F. Shafeichaharberoud, S. Lang, C. Whalen, C. Rivera Quiles, L. Purcell, C. Talbot, P. Wang, E. B. Norton, M. Mazei-Robison, A. Sulima, A. E. Jacobson, K. C. Rice, G. R. Matyas and X. Huang, *Bioconjugate Chem.*, 2024, **35**, 164–173.
- 46 Z. Tan, W. Yang, N. A. O'Brien, X. Pan, S. Ramadan, T. Marsh, N. Hammer, C. Cywes-Bentley, M. Vinacur, G. B. Pier, J. C. Gildersleeve and X. Huang, *Nat. Commun.*, 2024, **15**, 3420–3436.
- 47 J. Weber, H. Peng and C. Rader, *Exp. Mol. Med.*, 2017, **49**, e305.
- 48 S. U. Vetterli, K. Zerbe, M. Muller, M. Urfer, M. Mondal, S. Y. Wang, K. Moehle, O. Zerbe, A. Vitale, G. Pessi, L. Eberl, B. Wollscheid and J. A. Robinson, *Sci. Adv.*, 2018, **4**, eaau2634.
- 49 L. Kong, B. Vijayakrishnan, M. Kowarik, J. Park, A. N. Zakharova, L. Neiwert, A. Faridmoayer and B. G. Davis, *Nat. Chem.*, 2016, **8**, 242–249.

